

# Steering far-field spin-dependent splitting of light by inhomogeneous anisotropic media

Xiaohui Ling, Xinxing Zhou, Hailu Luo,\* and Shuangchun Wen†

Key Laboratory for Micro-/Nano-optoelectronic Devices of Ministry of Education,  
College of Information Science and Engineering, Hunan University, Changsha 410082, China  
(Dated: August 28, 2012)

An inhomogeneous anisotropic medium with specific structure geometry can apply tunable spin-dependent geometrical phase to the light passing through the medium, and thus can be used to steer the spin-dependent splitting (SDS) of light. In this paper, we exemplify this inference by the  $q$ -plate, an inhomogeneous anisotropic medium. It is demonstrated that when a linearly polarized light beam normally passes through a  $q$ -plate,  $k$ -space SDS first occurs, and then the real-space SDS in the far-field focal plane of a converging lens is distinguishable. Interestingly, the SDS, described by the normalized Stokes parameter  $S_3$ , shows a multi-lobe and rotatable splitting pattern with rotational symmetry. Further, by tailoring the structure geometry of  $q$ -plate or/and incident polarization angle of light, the lobe number and the rotation angle both are tunable. Our result suggests that the  $q$ -plate can serve as potential devices for manipulating the photon spin states and enable applications such as in nano-optics and quantum information.

PACS numbers: 42.25.-p, 42.60.Jf, 42.79.-e

## I. INTRODUCTION

Recent years, some fundamental effects in optics have attracted much attention, such as spin Hall effect of light [1, 2], optical Coriolis effect [3], and optical Magnus effect [4]. They manifest themselves as splitting of photon spin states, that is, when a linearly polarized light beam passes through a refractive index gradient (e.g., interfaces of different media) or an inhomogeneous medium, its left and right circular polarization components separate from each other. This spin-dependent splitting (SDS) effect is directly attributed to different geometrical phases that the two spin components respectively experienced, corresponding to the spin-orbital interaction [5, 6].

Light beam can acquire a spin-dependent geometrical phase upon the reflection or refraction of a refractive index gradient created by the interface of different media. When a linearly polarized paraxial light beam impinges obliquely upon this interface, the SDS in real space (coordinate space) generates, that is, the two spin components separate from each other and reside on both sides of the incident plane [5, 7–12]. This effect is known as the spin Hall effect of light, which has recently been extensively studied in other physical systems [13–18], in addition to optics. Actually, different refractive index gradients can give a light beam different geometrical phases, thereby result in specified switchable and enhanced SDS effects [11, 19]. Therefore, the geometrical phase can serve as an alternative tool for steering photon spin states. In general, real-space SDS is often accompanied with  $k$ -space (momentum space) SDS, associated with spin-dependent angular shift [20, 21]. Under normal incidence, both real-space and  $k$ -space splitting vanish due to the degeneracy of the geometrical phases of the two spin components [5].

While for some inhomogeneous anisotropic media, such as surface plasmonic nanostructures, plasmonic chains, and sub-

wavelength gratings [3, 22–24], even as under normal incidence, light beam can also acquire spin-dependent geometrical phases, and generates the SDS in the  $k$ -space. The real-space splitting can be induced after light propagating to the far field. Some recent researches have also shown that  $q$ -plate, a uniaxial birefringent waveplate with space-variant optical axis orientations, can give a beam  $\pm 2q$  topological charge and spin-dependent geometrical phases ( $q$  is an integer or a semi-integer) [25, 26]. Furthermore, tunable  $q$ -plates made by liquid crystals have been demonstrated to be conveniently realized, with arbitrary topological charge and geometrical phase [27–29]. Therefore, from this point of view, it would be interesting to explore the SDS effect in the  $q$ -plates as well as its potential ability to manipulate the photon spin states.

In this work, we theoretically show that  $q$ -plate can be employed to steer the SDS of light in the far field. This is due to that  $q$ -plate can apply a spin-dependent geometrical phase to a light beam that passes through it. And the geometrical phase is tunable by varying the  $q$ -plate geometry or incident linear polarization angle. When a linearly polarized light beam normally passes through the  $q$ -plate,  $k$ -space SDS first occurs. After converging by a lens, the induced real-space SDS in the far-field focal plane is distinguishable. The normalized Stokes parameter  $S_3$  is employed to reveal the separation of spin photons, because  $S_3$  represents the circular polarization degree of light [30]. We find that the spatial distribution of  $S_3$  exhibits a multi-lobe and rotatable splitting pattern with rotational symmetry. Further, by tailoring the structure geometry of  $q$ -plate or/and incident polarization angle of light, the lobe number and the rotation angle both are tunable. Note that as the light beam impinges normally into the  $q$ -plate, the birefringence does not induce the separation of ordinary and extraordinary light, which will not contribute to the SDS effect.

## II. MODEL AND THEORY

The  $q$ -plate is essentially a uniaxial birefringent waveplate with locally varying optical axis (fast or slow) orientations in the transverse  $xy$  plane, having a homogeneous phase retar-

\*Electronic address: hailulu@hnu.edu.cn

†Electronic address: scwen@hnu.edu.cn

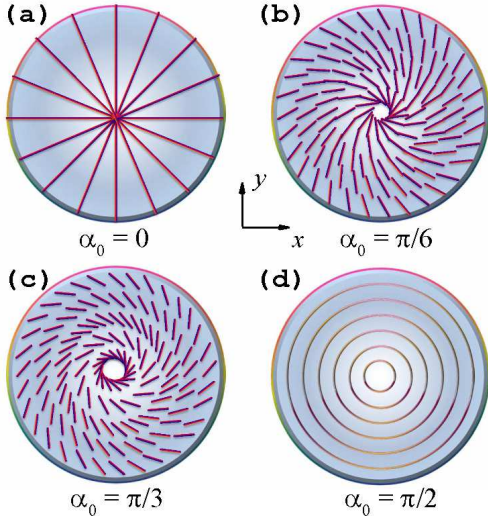


FIG. 1: (Color online) Examples of the  $q$ -plate geometries for  $q=1$ . The tangent to the lines shown indicates the local optical axis orientation (fast axis). (a)-(d) represent the geometries for  $\alpha_0=0, \pi/6, \pi/3$ , and  $\pi/2$ , respectively.

dation  $\Phi = 2\pi(n_e - n_o)d/\lambda$  with  $n_e$ ,  $n_o$ ,  $d$ , and  $\lambda$  the refractive indices of slow and fast waves, material thickness, and operation wavelength, respectively. It can be currently realized using liquid crystals, sub-wavelength gratings, or polymers [22, 25, 31]. The fast axis orientations, as specified by a space-variant angle  $\alpha(x, y)$  it forms with the  $x$ -axis, are described by the following equation:

$$\alpha(x, y) = q \arctan\left(\frac{y}{x}\right) + \alpha_0, \quad (1)$$

where  $q$  is an integer or semi-integer,  $\alpha_0$  indicates the angle of local optical axis direction forming with the local radial direction. Figure 1 shows four geometries of  $q = 1$  when  $\alpha_0=0, \pi/6, \pi/3$ , and  $\pi/2$ .

The Jones matrix, describing a uniaxial crystal with fast axis in the  $x$ -direction, can be represented as [30]

$$J = \begin{bmatrix} t_x \exp(i\Phi/2) & 0 \\ 0 & t_y \exp(-i\Phi/2) \end{bmatrix}, \quad (2)$$

where  $t_x$  ( $t_y$ ) is the transmission coefficient in  $x$  ( $y$ )-direction.

As the  $q$ -plate has space-variant optical axis orientations, a position-dependent Jones matrix  $T(x, y)$  can be employed to fully characterize the light propagation through the  $q$ -plate [25, 30]:

$$\begin{aligned} T(x, y) &= R(-\alpha)JR(\alpha) \\ &= \frac{t_x e^{i\Phi/2} + t_y e^{-i\Phi/2}}{2} \begin{pmatrix} 1 & 0 \\ 0 & 1 \end{pmatrix} \\ &\quad + \frac{t_x e^{i\Phi/2} - t_y e^{-i\Phi/2}}{2} \begin{pmatrix} \cos 2\alpha & \sin 2\alpha \\ \sin 2\alpha & -\cos 2\alpha \end{pmatrix}, \end{aligned} \quad (3)$$

where

$$R(\alpha) = \begin{pmatrix} \cos \alpha & \sin \alpha \\ -\sin \alpha & \cos \alpha \end{pmatrix}.$$

An input linearly polarized light, with its electric field described by a Jones vector, is given as

$$E_{in}(x, y) = \begin{pmatrix} \cos \theta \\ \sin \theta \end{pmatrix} E_0(x, y). \quad (4)$$

Here,  $\theta$  is the linear polarization angle of the polarization vector forming with the  $x$ -axis; see Fig. 2. Let  $E_0(x, y)$  be a collimated Gaussian beam:  $E_0(x, y) = \exp[-(x^2 + y^2)/w_0^2]$  with  $w_0$  the beam waist. For simplicity, we neglect the absorption and loss, and let  $t_x$  and  $t_y$  both be equal to 1. Then, the output electric field,  $E_{out}(x, y) = T(x, y)E_{in}(x, y)$ , can be calculated as

$$\begin{aligned} E_{out}(x, y) &= \frac{1}{2} e^{-i\theta} \left[ \cos \frac{\Phi}{2} + i \sin \frac{\Phi}{2} e^{-i\varphi} \right] \begin{pmatrix} 1 \\ i \end{pmatrix} E_0 \\ &\quad + \frac{1}{2} e^{i\theta} \left[ \cos \frac{\Phi}{2} + i \sin \frac{\Phi}{2} e^{i\varphi} \right] \begin{pmatrix} 1 \\ -i \end{pmatrix} E_0, \end{aligned} \quad (5)$$

where

$$\varphi = 2\alpha(x, y) - 2\theta = 2[q \arctan(y/x) + \alpha_0 - \theta] \quad (6)$$

is an additional space-variant geometrical phase [32, 33], depending on the local optical axis orientation of the  $q$ -plate.  $E_{out}(x, y)$  consists of two parts, corresponding to a coherent superposition of left and right circular polarization components, each of which is respectively composed of two terms: one carries a space-variant geometrical phase ( $\pm\varphi$ ) and  $\pm 2q$  topological charge, and the other does not. This originates from the partially conversion of spin-to-orbital angular momentum, with the conversion efficiency determined by  $\Phi$  [27]. Actually, as the incident beam is linearly polarized, partial left-handed photons transform into right-handed photons and acquire an additional angular momentum ( $+2q\hbar$ ) to keep the total angular momentum conserved, and vice versa [25–27]. Generally, the spin-orbital interaction is the origin of such fundamental effects as the spin Hall effect of light, optical Coriolis effect and optical Magnus effect, which manifest as SDS phenomenon. Thus here, under normal incidence of a linearly polarized light,  $k$ -space SDS will first occur, and then real-space SDS upon propagation. Note that  $\varphi$  involves three free

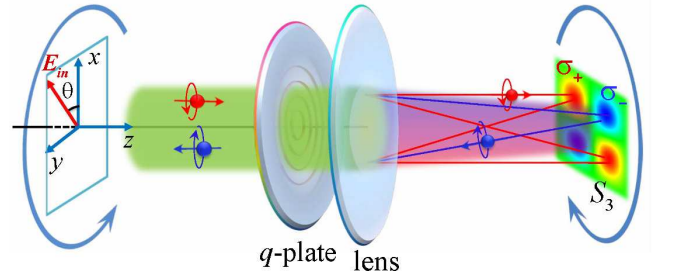


FIG. 2: (Color online) Schematic illustrating the SDS produced by a  $q$ -plate. A linearly polarized light beam normally passes through the  $q$ -plate, and is focused by a lens.  $\sigma_+$  and  $\sigma_-$  represent the left and right circular polarization components, respectively. The two curves with arrows indicate that the splitting patterns will rotate when rotating the incident polarization direction ( $\theta$ ). The additional devices for measuring the Stokes parameter  $S_3$  are not shown.

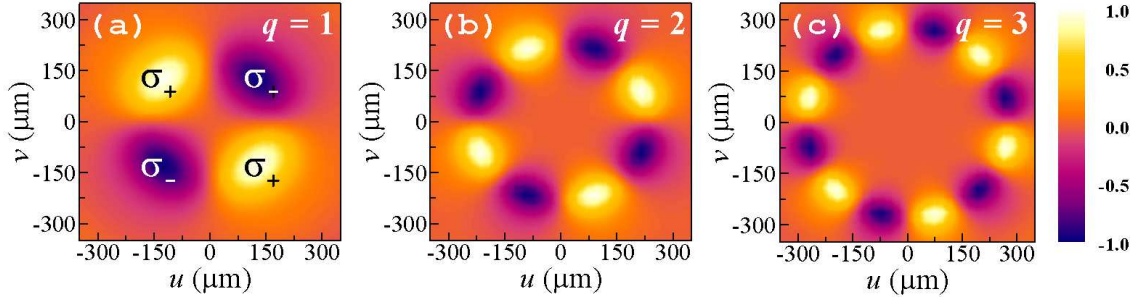


FIG. 3: (Color online) Normalized Stokes parameter  $S_3$  in the focal plane under the irradiation of a linearly  $x$ -polarized light for (a)  $q=1$ , (b)  $q=2$ , and (c)  $q=3$ , respectively. Here,  $\alpha_0 = 0$ . In the calculations, we set  $\Phi = \pi/2$ ,  $\lambda = 1 \mu\text{m}$ ,  $w_0 = 1 \text{ mm}$ , and  $f_0 = 0.5 \text{ m}$ .

parameters:  $q$ ,  $\alpha_0$ , and  $\theta$ , which serves as effective ways for manipulating the SDS of light.

The momentum shift of the SDS then can be calculated as [3, 22–24]

$$\begin{aligned} \Delta k &= -\sigma_{\pm} \nabla \varphi = \Delta k_x + \Delta k_y \\ &= 2\sigma_{\pm} q \left( \frac{y}{x^2 + y^2} \hat{e}_x + \frac{-x}{x^2 + y^2} \hat{e}_y \right), \end{aligned} \quad (7)$$

where  $\sigma_+ = +1$  and  $\sigma_- = -1$ , representing the left and right circular polarization components, respectively, and  $\hat{e}_x$  ( $\hat{e}_y$ ) is the unit vector in  $x$  ( $y$ )-direction.  $\Delta k_x$  and  $\Delta k_y$  are position-dependent, with shift directions respectively determined by their signs. As the geometrical phase of the  $q$ -plate is space-variant both in  $x$ - and  $y$ -directions, the  $k$ -space SDS and shift in both directions occur simultaneously. Unlike this, a recent work have reported a constant momentum shift in plasmonic chains where the SDS effect occurred in one direction [24].

### III. TUNABLE SPIN-DEPENDENT SPLITTING IN THE FAR FIELD

We then consider the far-field SDS effect. A lens with focal length  $f_0$  is used here to converge the output field of  $q$ -plate, and the field in the focal plane can be viewed as far field, as schematically shown in the Fig. 2. The real-space shift induced by the SDS in the focal plane can be written as  $\Delta S = \lambda f_0 \Delta k / 2\pi$  [34]. It is also position-dependent, which means each point in the  $q$ -plate contributes a different momentum shift; thereby, in the far field, the final splitting effect is determined by their coherent superposition.

The electric field distribution in the focal plane can be derived from the Fraunhofer-diffraction integral formula [35]:

$$\begin{aligned} E_{out}^{u(v)}(u, v) &= \frac{\exp(ik_0 f_0) \exp\left[\frac{ik_0}{2f_0}(u^2 + v^2)\right]}{i\lambda f_0} \iint_{S_{\alpha\beta}} dx dy \\ &\quad \times E_{out}^{x(y)}(x, y) \exp\left[-\frac{ik_0}{f_0}(xu + yv)\right], \end{aligned} \quad (8)$$

where  $u$  and  $v$  are axes parallel to the  $x$  and  $y$  axes, respectively,  $S_{\alpha\beta}$  is the space range of the  $q$ -plate, and  $E_{out}^{x(y)}(x, y)$  represents the  $x$  ( $y$ )-polarized component of  $E_{out}(x, y)$ . As this

integral is too complicated to solve analytically, we will evaluate it numerically.

In order to show the circular polarization degree of the resulting electric field and reveal the separation of spin photons, the Stokes parameter  $S_3$  is employed. Describing the SDS by  $S_3$  is believed to be as the photonic version of a Stern-Gerlach experiment in the absence of a magnetic field [23, 36]. The  $S_3$ , normalized to the total intensity in the focal plane, can be calculated as [30]

$$S_3 = \frac{2|E_{out}^u(u, v)||E_{out}^v(u, v)| \sin(\psi_v - \psi_u)}{|E_{out}^u(u, v)|^2 + |E_{out}^v(u, v)|^2}, \quad (9)$$

where  $\psi_{u(v)}$  is the phase of  $E_{out}^{u(v)}(u, v)$  and the denominator represents the total intensity in the focal plane.

We now can demonstrate the SDS in the far field produced by the  $q$ -plates. As stated above, the far-field SDS of left and right circular polarization components results from their spin-dependent geometrical phase experienced in the  $q$ -plate. Since the geometrical phase is space-variant,  $S_3$  parameter is inhomogeneous in the far-field focal plane. Note that  $\varphi$  involves three tunable parameters:  $q$ ,  $\alpha_0$ , and  $\theta$ , we will then ex-

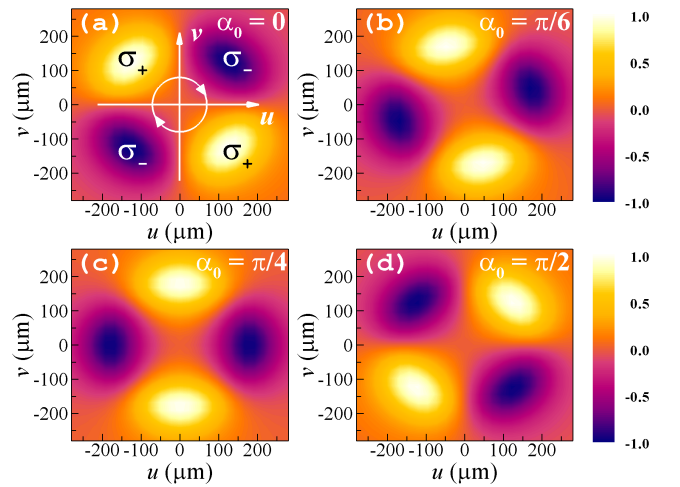


FIG. 4: (Color online) Normalized Stokes parameter  $S_3$  in the focal plane under the irradiation of a linearly  $x$ -polarized light for (a)  $\alpha_0 = 0$ , (b)  $\alpha_0 = \pi/6$ , (c)  $\alpha_0 = \pi/4$ , and (d)  $\alpha_0 = \pi/2$ , respectively. Other parameters are the same as in Fig. 3. The white arrows shows the clockwise rotation of  $S_3$  with the increase of  $\alpha_0$ .

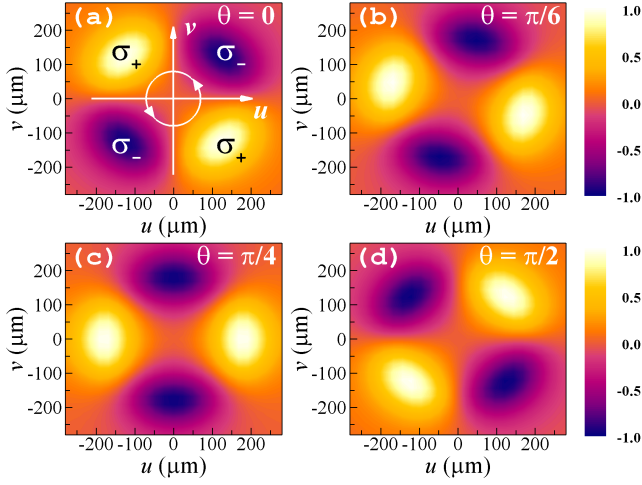


FIG. 5: (Color online) Normalized Stokes parameter  $S_3$  in the focal plane under the irradiation of a linear polarization light with polarization angle (a)  $\theta = 0$ , (b)  $\theta = \pi/6$ , (c)  $\theta = \pi/4$ , and (d)  $\theta = \pi/2$ , respectively. Here,  $\alpha_0 = 0$ . Other parameters are the same as in Fig. 3. The white arrows shows the counterclockwise rotation of  $S_3$  with the increase of  $\theta$ .

plore the influence of these parameters on the SDS. The first two parameters are associated with changing the  $q$ -plate geometry, and the third one is just related to change the incident linear polarization angle which may be more conveniently to adjust.

We first discuss the influence of the  $q$  value on SDS. Figure 3 shows the spatial distribution of the calculated  $S_3$  parameter for  $q = 1, 2, 3$  ( $\alpha_0 = 0$ ) under the linearly  $x$ -polarized incidence ( $\theta = 0$ ). It is well known that  $S_3 > 0$  corresponds to left-handed polarization helicity and  $S_3 < 0$  corresponds to right-handed polarization helicity. Especially,  $S_3 = +1$  or  $-1$  corresponds to  $\sigma_+$  or  $\sigma_-$  [30]. One can notice that, for  $q = 1, 2, 3$ , the spatial distributions of  $S_3$  show 4, 8, 12 independent lobes, respectively, with alternative  $\sigma_+$  and  $\sigma_-$  components. Moreover, the  $S_3$  exhibits twofold rotational ( $C_2$ ) symmetry for  $q = 1$ , fourfold rotational ( $C_4$ ) symmetry for  $q = 2$ , and sixfold rotational ( $C_6$ ) symmetry for  $q = 3$ , respectively. These characteristics are determined by the rotational symmetric geometries of the  $q$ -plate and the geometrical nature of the space-variant geometrical phase [Eq. (6)]. Interestingly, similar four-lobe spin splitting effect has also been observed in semiconductor microcavities for exciton polaritons [13–15] and subwavelength metallic apertures for photons [36], which corresponds to the case of  $q = 1$ .

Here, we can give a qualitative explanation for this interesting SDS phenomenon. Note that the output electric field of the  $q$ -plate have two parts with opposite spin handedness and topological charge ( $\pm 2q$ ), that is, two helical circular polarization beams [see Eq. (5)]. The wavefront of helical beam with  $\pm 2q$  topological charge is composed of  $2|q|$  intertwined helical surfaces, with their handedness determined by the sign of  $2q$  [25]. After interfering and propagating to the far-field focal

plane, these helical surfaces form  $4|q|$  independent lobes with alternative  $\sigma_+$  and  $\sigma_-$  components, which can be described by the  $S_3$  parameter.

Nonvanishing  $\alpha_0$  and  $\theta$  will cause the rotation of the spatial distribution of  $S_3$ , since they both can give an initial value to the geometrical phase  $\varphi$ . We take  $q = 1$  for an example to show the influence of  $\alpha_0$  and  $\theta$  on the SDS. As  $\alpha_0$  and  $\theta$  play similar roles in the geometrical phase with just opposite signs, their influences will cancel out each other. When  $\theta = 0$ , increasing  $\alpha_0$  will result in the clockwise rotation of  $S_3$  for  $\alpha_0$  radian, as shown in Fig. 4. Accordingly, increasing  $\theta$  under the condition of  $\alpha_0 = 0$  will make  $S_3$  rotate counterclockwise for  $\theta$  radian (see Fig. 5). Obviously,  $\alpha_0$  and  $\theta$  produce the same rotation angles but opposite rotation directions. These results confirm the predications.

In the above calculations, we have assumed that the  $q$ -plate served as a quarter waveplates ( $\Phi = \pi/2$ ) with space-variant optical axis orientations. It's worth noting that, actually, the SDS does not occur for all cases of  $\Phi$ . When  $\Phi = 2m\pi$  ( $m$  is an integer), the term carrying geometrical phase in Eq. (5) vanishes, and the rest part represents a field with the same polarization as the incident light, that is, no SDS occur. When the  $q$ -plate serves as a half waveplate ( $\Phi = n\pi$ ,  $n$  is an odd number),  $E_{out}(x, y) = i[\cos(2\alpha - \theta), \sin(2\alpha - \theta)]^T E_0$ , which represents a linearly polarized light beam with axisymmetric polarization distribution [37]. Thus, for these cases, the SDS vanishes.

#### IV. CONCLUSIONS

We have demonstrated a tunable SDS effect in the far field produced by the inhomogeneous anisotropic media with specified geometries, called  $q$ -plate, under normal incidence of a linearly polarized light. This effect originates from the spin-dependent geometrical phases of the two spin components experienced in the  $q$ -plate. We have also shown that the SDS, described by  $S_3$  parameter, exhibits a multi-lobe and rotatable splitting pattern, with the lobe number and rotation angle tunable by the geometrical phase (associated with  $q$ -plate geometry and the incident linear polarization angle). As the  $q$ -plate with arbitrary geometrical phase could be achieved by the current fabrication technology using liquid crystals, sub-wavelength gratings, or polymers, we believed that it will serve as a potential device for manipulating the photon spin states and enables applications, such as in nano-optics and quantum information.

#### Acknowledgments

This work was supported by the National Natural Science Foundation (Grants No. 61025024 and 11074068) and Hunan Provincial Natural Science Foundation (Grant No. 12JJ7005) of China.

- 
- [1] M. Onoda, S. Murakami, and N. Nagaosa, Phys. Rev. Lett. **93**, 083901 (2004).
  - [2] K. Y. Bliokh and Y. P. Bliokh, Phys. Rev. Lett. **96**, 073903 (2006).
  - [3] K. Y. Bliokh, Y. Gorodetski, V. Kleiner, and E. Hasman, Phys. Rev. Lett. **101**, 030404 (2008).
  - [4] A. V. Dooghin, N. D. Kundikova, V. S. Liberman, and B. Ya. Zel'dovich, Phys. Rev. A **45**, 8204 (1992).
  - [5] O. Hosten and P. Kwiat, Science **319**, 787 (2008).
  - [6] K. Y. Bliokh, A. Niv, V. Kleiner, and E. Hasman, Nat. Photon. **2**, 748 (2008).
  - [7] A. Aiello and J. P. Woerdman, Opt. Lett. **33**, 1437 (2008).
  - [8] H. Luo, S. Wen, W. Shu, Z. Tang, Y. Zou, and D. Fan, Phys. Rev. A **80**, 043810 (2009).
  - [9] Y. Qin, Y. Li, X. Feng, Z. Liu, H. He, Y.-F. Xiao, and Q. H. Gong, Opt. Express **18**, 16832 (2010).
  - [10] N. Hermosa, A. M. Nugrowati, A. Aiello, and J. P. Woerdman, Opt. Lett. **36**, 3200 (2011).
  - [11] H. Luo, X. Zhou, W. Shu, S. Wen, and D. Fan, Phys. Rev. A **84**, 043806 (2011).
  - [12] X. Zhou, Z. Xiao, H. Luo, and S. Wen, Phys. Rev. A **85**, 043809 (2012).
  - [13] A. Kavokin, G. Malpuech, and M. Glazov, Phys. Rev. Lett. **95**, 136601 (2005).
  - [14] C. Leyder, M. Romanelli, J. Ph. Karr, E. Glacabino, T. C. H. Liew, M. M. Glazov, A. V. Kavokin, G. Malpuech, and A. Bramati, Nat. Phys. **3**, 628 (2007).
  - [15] M. Maragkou, C. E. Richards, T. Ostatnický, A. J. D. Grundy, J. Zajac, M. Hugues, W. Langbein, and P. G. Lagoudakis, Opt. Lett. **36**, 1095 (2011).
  - [16] J.-M. Ménard, A. E. Mattacchione, H. M. van Driel, C. Hautmann, and M. Betz, Phys. Rev. B **82**, 045303 (2010).
  - [17] P. Gosselin, A. Bérard, and H. Mohrbach, Phys. Rev. D **75**, 084035 (2007).
  - [18] C. A. Dartora, G. G. Cabrera, K. Z. Nobrega, V. F. Montagner, M. H. K. Matielli, F. K. R. de Campos, and H. T. S. Filho, Phys. Rev. A **83**, 012110 (2011).
  - [19] H. Luo, X. Ling, X. Zhou, W. Shu, S. Wen, and D. Fan, Phys. Rev. A **84**, 033801 (2011).
  - [20] H. Luo, S. Wen, W. Shu, and D. Fan, Phys. Rev. A **82**, 043825 (2010).
  - [21] X. Zhou, H. Luo, and S. Wen, Opt. Express **20**, 16003 (2012).
  - [22] A. Niv, Y. Gorodetski, V. Kleiner, and E. Hasman, Opt. Lett. **33**, 2910 (2008).
  - [23] Y. Gorodetski, A. Niv, V. Kleiner, and E. Hasman, Phys. Rev. Lett. **101**, 043903 (2008).
  - [24] N. Shitrit, I. Bretner, Y. Gorodetski, V. Kleiner, and E. Hasman, Nano Lett. **11**, 2038 (2011).
  - [25] L. Marrucci, C. Manzo, and D. Paparo, Phys. Rev. Lett. **96**, 163905 (2006).
  - [26] L. Marrucci, E. Karimi, S. Slussarenko, B. Piccirillo, E. Santamato, E. Nagali, and F. Sciarrino, J. Opt. **13**, 064001 (2011).
  - [27] S. Slussarenko, A. Murauski, T. Du, V. Chigrinov, L. Marrucci, and E. Santamato, Opt. Express **19**, 4085 (2011).
  - [28] E. Karimi, B. Piccirillo, E. Nagali, L. Marrucci, and E. Santamato, Appl. Phys. Lett. **94**, 231124 (2009).
  - [29] B. Piccirillo, V. D'Ambrosio, S. Slussarenko, L. Marrucci, and E. Santamato, Appl. Phys. Lett. **97**, 241104 (2010).
  - [30] A. Yariv and P. Yeh, *Photonics: Optical Electronics in Modern Communications* (Oxford University Press, New York, 2007).
  - [31] S. Nersisyan, N. Tabiryan, D. M. Steeves, and B. R. Kimball, Opt. Express **17**, 11926 (2009).
  - [32] Z. Bomzon, G. Biener, V. Kleiner, and E. Hasman, Opt. Lett. **27**, 1141 (2002).
  - [33] E. Hasman, G. Biener, A. Niv, and V. Kleiner, Prog. Opt. **47**, 215 (2005).
  - [34] Y. Gorodetski, G. Biener, A. Niv, V. Kleiner, and E. Hasman, Opt. Lett. **30**, 2245 (2005).
  - [35] J. W. Goodman, *Introduction to Fourier Optics* (3rd Edition) (Roberts, 2005).
  - [36] M. Kang, J. Chen, B. Gu, Y. Li, L. T. Vuong, and H.-T. Wang, Phys. Rev. A **85**, 035801 (2012).
  - [37] M. Stalder and M. Schadt, Opt. Lett. **21**, 1948 (1996).